










Enhancement of corrosion protection of metal carbon steel C45 and stainless steel 316 by using inhibitor (Schiff base) in sea water

Mazin Hasan Raheema ^{*1}  , Noor Ali Khudhair ²  , Taghreed H. AL-Noor ³  ,
Salam R Al-Ayash ³  , Hussian H. Kharnoob ⁴   and Shatha M. H. Obed ³  

¹Department of Dentistry, University Al-Turath College, Baghdad, Iraq.

²Department of Chemistry, College of Science, University of Baghdad, Baghdad, Iraq.

³Department of Chemistry, Ibn-Al-Haithem of College of Education for Pure Science, University of Baghdad, Baghdad, Iraq.

⁴Department of Anesthesia and Intensive Care, University Al-Turath College, Baghdad, Iraq.

*Corresponding Author.

Received 13/09/2022, Revised 14/02/2023, Accepted 16/02/2023, Published 20/06/2023



This work is licensed under a [Creative Commons Attribution 4.0 International License](https://creativecommons.org/licenses/by/4.0/).

Abstract

This research has presented a solution to the problem faced by alloys: the corrosion problem, by reducing corrosion and enhancing protection by using an inhibitor (Schiff base). The inhibitor (Schiff base) was synthesized by reacting of the substrates materials (4-dimethylaminobenzaldehyde and 4-aminoantipyrine). It was diagnosed by infrared technology IR, where the IR spectrum and through the visible beams proved that the Schiff base was well formed and with high purity. The corrosion behavior of carbon steel and stainless steel in a saline medium (artificial seawater 3.5%NaCl) before and after using the inhibitor at four temperatures: 20, 30, 40, and 50 C° was studied by using three electrodes potentiostat. The corrosion behavior was studied by cathode and anode polarization through which all corrosion parameters were investigated which include: corrosion current i_{corr} (1341×10^{-7} - 5393×10^{-9} A/cm²), corrosion potential E_{corr} (-1.031- -0.227 mV vs SCE) , corrosion rates CR (0.658-0.007 mm.y⁻¹), inhibition efficiency %IE (92-98%), and energy activation barriers E_a (4.709-26.733 kJ/mole). The thermodynamic and kinetic properties of the corrosion behavior of these two metals under study, which include: enthalpy ΔH^* (2.153-24.176 kJ/mole), entropy ΔS^* (-197 -156 J/mole), and free Gibbs energy ΔG^* (59.87-74.56 kJ/mole) before and after using the inhibitor, were also studied.

Keywords: Corrosion inhibition, Carbon steel, Inhibitor, Schiff base, Stainless steel.

Introduction

Corrosion can be defined briefly as an electrochemical reaction that occurs between the metal and the environment, which leads to the loss and destruction of part of the metal. The Corrosive environment is either in the form of liquids or the form of air and gases, so it can be classified into two types, namely, wet corrosion where the corrosive environment is liquid (ie the environment

is brine, acidic solutions, alkaline solutions or water) and dry corrosion, where the corrosive environment is a dry gas and is usually called chemical corrosion¹. The effect of corrosion on the surface of the metal takes several forms depending on the state, nature, and conditions of the corrosive environment which causes metal corrosion, therefore, it can be classified into several types;

Uniform (general) corrosion, galvanic (Metal-Metal) corrosion, pitting corrosion, selective corrosion, crevice corrosion, intergranular corrosion, stress corrosion cracking, erosion

corrosion². Corrosion processes can be explained briefly, as they are considered part of the electrochemical processes, which are illustrated in the Fig. 1 below:

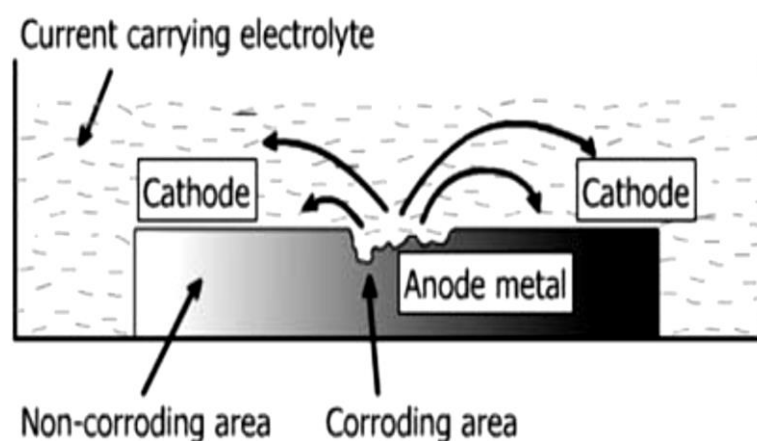


Figure 1. Corrosion cell².

The Fig. 1, above shows us the oxidation and reduction reactions that occur at the anode and cathode electrodes, respectively.

Resorting to solving the corrosion problem has attracted great interest from many researchers, as there are several methods used to reduce corrosion that affect alloys, including the use of corrosion-resistant materials, and there are two ways to use those materials that are resistant to corrosion to reduce corrosion and enhance protection; the first is the use of the coating method, which is coating these materials on the surface of the metal and making a thin layer on its surface that acts as an insulating layer that isolates the metal surface from the corrosive surroundings as much as possible and through physical adsorption. Recently, nanomaterials have been used as a coating material on metal surfaces because of the unique properties that distinguish them from other materials. The most important of these materials are TiO₂, ZnO, Al₂O₃, ZrO₂...etc³⁻⁵, nanopolymers⁶⁻⁸, carbon nanomaterials (as reduced graphene oxide, graphene, and carbon nanotubes)⁹⁻¹², drugs¹³⁻¹⁶, and environmentally friendly materials¹⁷ all of which are reported. The second method that is used to reduce corrosion is the use of the so-called

corrosion inhibitors¹⁸, which are chemical compounds, especially organic compounds (drugs or ligands; Especially ligands that contain nitrogen atoms¹⁹⁻²¹, such as Schiff bases²²⁻²⁵ or other ligands²⁶⁻²⁹) or nanoparticles³⁰, that are added in small concentrations to the corrosion medium, they reduce corrosion by decreasing cathodic reduction or anodic oxidation, or both, by making a film on the metal surface. It is assumed that the adsorption of inhibitors on the surface of the metal is either through physical adsorption or chemical adsorption³¹. There is a lot of research in this field has been recorded. In this work, Schiff base was used as an inhibitor for several reasons, including: The adsorption of inhibitors occurs through the presence of heteroatoms such as nitrogen, oxygen, phosphorus and sulfur. The inhibition efficiency of these heteroatom's have been reported to follow the sequence O<N<S<P^{32,33}. Now days, the condensation products of aldehydes or ketones with amines i.e., Schiff base have been reported with good inhibitive properties. These are the important class of ligands in co-ordination chemistry. This ability is due to the presence of C=N groups. Schiff bases become effective by adsorption on the metal/solution surface and protect it from the hazardous effect of saline media.

Materials and Methods

Preparation of inhibitor (Schiff base)

All chemicals used were of reagent grade (supplied by either Merck and Fluka, and used as supplied.

Schiff base was previously prepared and mentioned³⁴.

The Schiff base was prepared from the reaction of 4-dimethylaminobenzaldehyde with 4-aminoantipyrine as follows:

First, the reactants were dissolved in methanol solvent (1 mmol \ 0.149 g) of (4-dimethylaminobenzaldehyde was dissolved in

15mL methanol and (1 mmol/0.203 g) of (4-aminoantipyrine) was dissolved in 10mL methanol. After that, in a round flask, the reactants were added with the addition of two drops of glacial acetic acid, and the mixture was left with continuous stirring for two hours, after the completion of the reaction period, yellow crystals are formed. The Product was collected by filtration, washed several times with ethanol and recrystallized from hot ethanol and air dried. The Fig.2, below shows the chemical reaction preparation of the Schiff base.

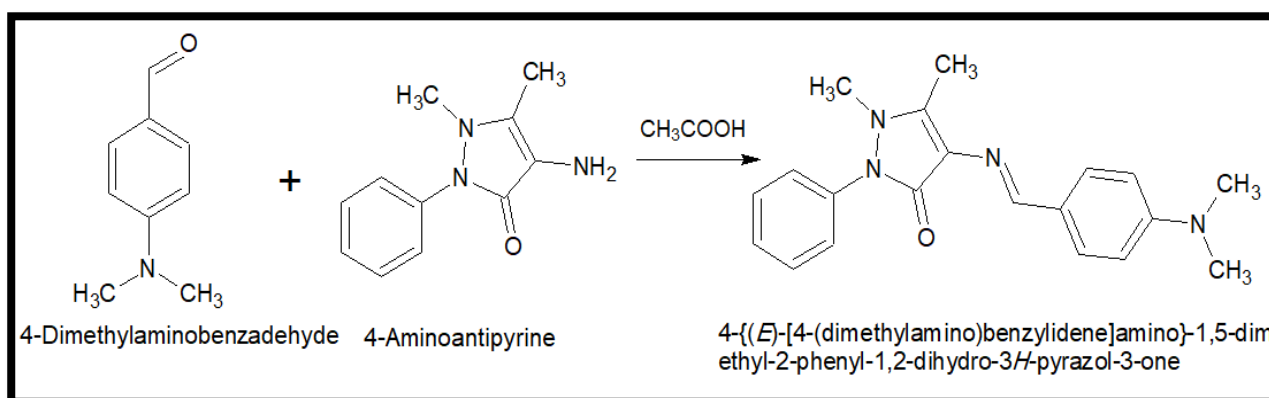


Figure 2. Preparation of the Schiff base³⁴.

Corrosion measurement

The corrosion tests (as shown in Fig.3, and Fig.4) were conducted with the use of an advanced potentiostat with all accessories of the cell body made of Pyrex consisting of internal and external bowls, a host computer, thermostat, magnetic stirrer, electrodes (reference electrode, auxiliary electrode working electrode) and working electrode holder. The corrosive media was artificial seawater 3.5% NaCl prepared by dissolving 35 gm of sodium chloride in 1000 mL deionized water, the inhibitor solution was prepared by dissolving 10 mg of the inhibitor in 100 mL (50% dimethylformamide (DMF)+ 50% deionized water) 100 ppm (The concentration of the inhibitor is directly proportional to the inhibition efficiency, that is, the higher the concentration of the inhibitor, the greater

the inhibition efficiency). The two metals under study were made in a circular shape with a diameter of 2.5 cm and a thickness of 1 mm and were polished by silicon carbide (SiC) grit abrasive paper from 400, 600, 800, 1200 and 2000, then they were washed with acetone and distilled water DW and with ethanol, then, they were introduced into desiccators to prevent their oxidation (the Table 1 below shows the chemical composition of the two metals, carbon steel, and stainless steel). The polarization curves (Tafel plots) were scanned between -200 to + 200 mv from the open circuit potential and the corrosion currents (i_{cor}) plus the corrosion potentials (E_{cor}) of the metals under study (before and after using inhibitor) 50 ml of inhibitor was added, which were estimated by extrapolating the cathodic and anodic Tafel lines at four different temperatures of 20, 30, 40, and 50°C.

Table 1. Chemical composition of carbon steel and stainless steel used in this work.

Stainless steel		C45 Carbon steel	
Element	% Weight	Element	% Weight
C	0.08	C	0.36-0.42
Si	0.75	Si	0.15-0.30
Mn	2.00	Mn	1.00-1.40
S	0.03	S	0.05
P	0.045	P	0.05
Cr	18.00	Cr	0.20
Ni	14.00	Ni	0.20
Fe	61.99	Fe	97.49
N	0.10		
Mo	3.00		

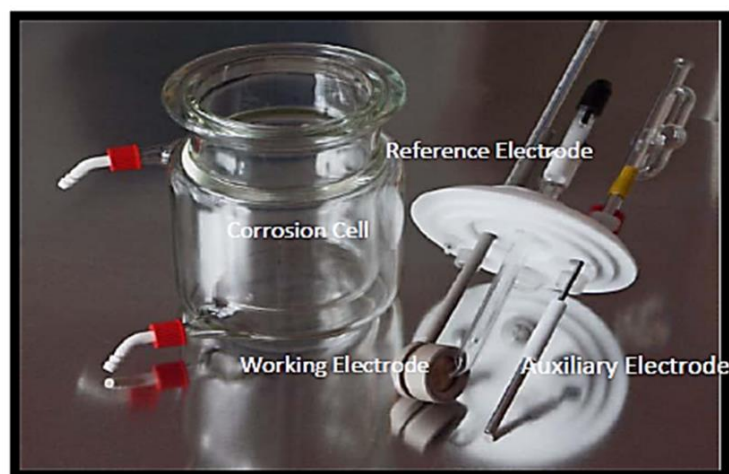


Figure 3. Set up the corrosion cell and three electrodes.

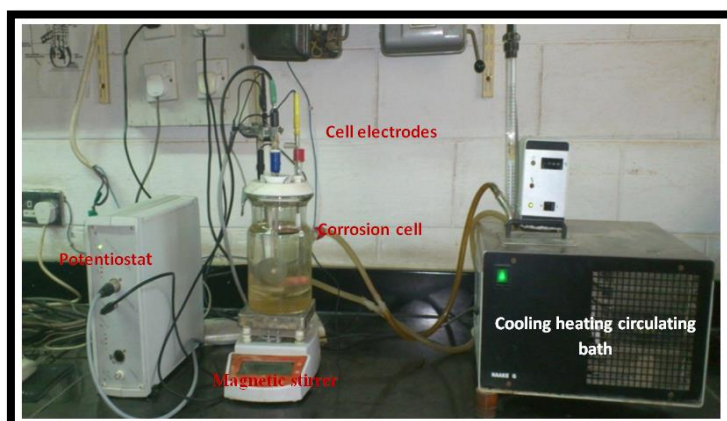


Figure 4. Potentiostat corrosion rate measurement apparatus.

Results and Discussion

Schiff base characterization

The prepared Schiff base was diagnosed by Fourier Transform Infrared Spectrophotometer, as well as the substrates materials from which the Schiff base was prepared for comparison (as shown in Figs. 5, 6, and 7. In general, the band at 1608.63 cm^{-1} belongs to the azomethine group $\nu(\text{HC}=\text{N}-)$, which is present in the prepared Schiff base and its absence in the substrates materials from which the Schiff base was prepared, and this indicates the formation of the Schiff base and the two bands at

3433 cm^{-1} and 3325 cm^{-1} belong to the amine group $\nu(\text{NH}_2)$, which appeared in 4-aminoantipyrene (the basic material from which the Schiff base was prepared) and disappeared in the Schiff base this indicates the formation of the azomethine $\nu(\text{HC}=\text{N}-)$ group and thus indicates the formation of a Schiff base. The bands at (1647, 1662, and 1647.21) cm^{-1} belong to the carbonyl group $\nu(\text{C}=\text{O})$ of the compounds 4-aminoantipyrene, 4-dimethylaminobenzaldehyde, and prepared Schiff base, respectively.

11/23/2022 11:59:57 AM

BPC-Analysis Center

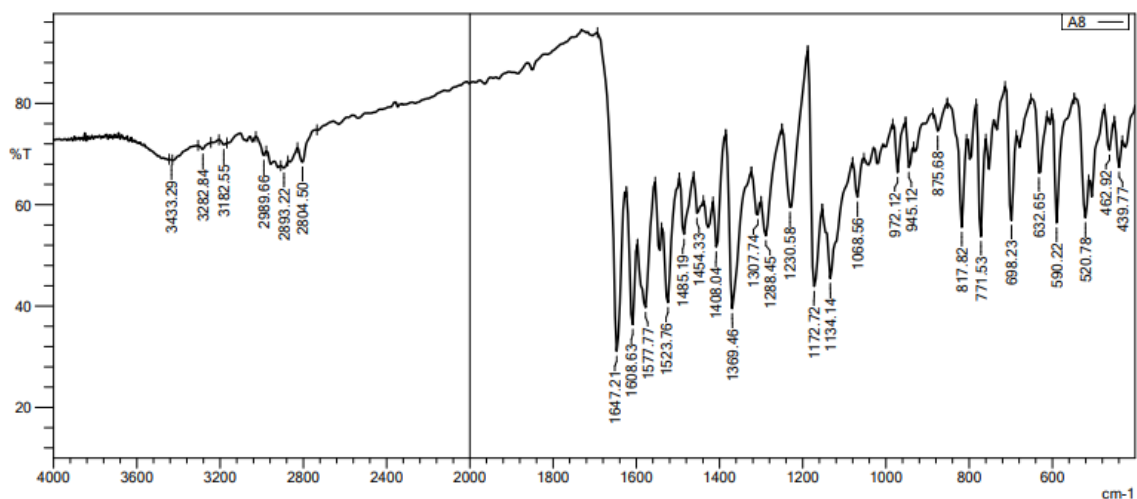


Figure 5. The (FTIR) Spectrum of prepared Schiff base.

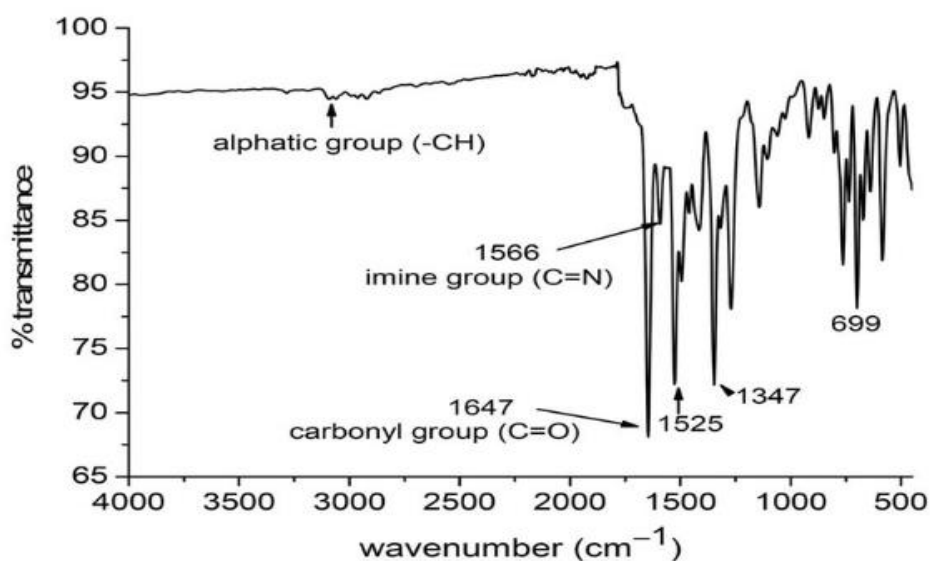


Figure 6. The (FTIR) Spectrum of 4-aminoantipyrene.

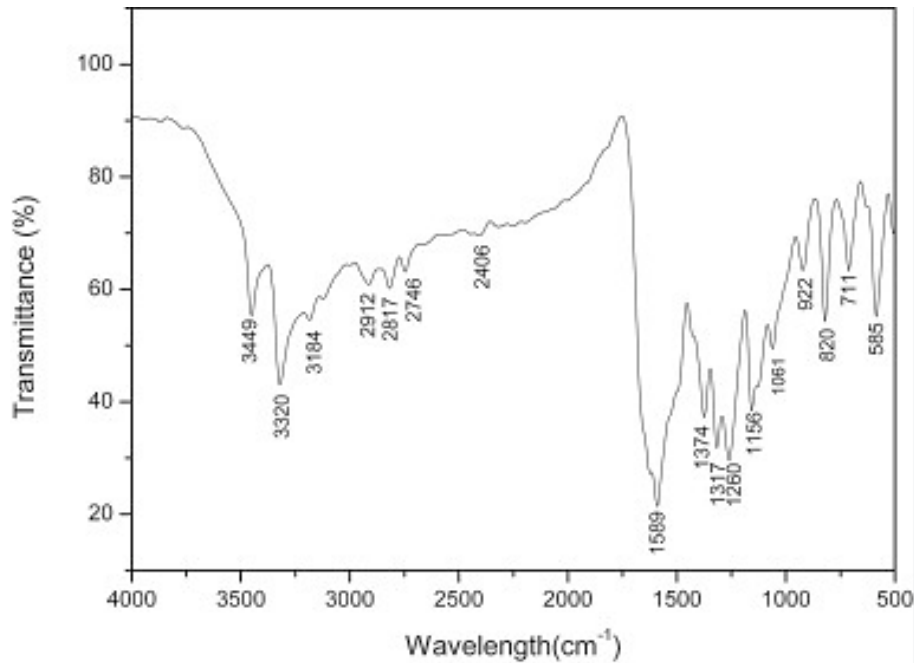


Figure 7. The (FTIR) Spectrum of 4-dimethylaminobenzaldehyde.

Corrosion Parameters Measurement

From the Tafel polarization curves (Tafel plots shown in Figs. 8, 9, 10, and 11) the corrosion parameters were calculated which include: The corrosion current density (i_{corr}), corrosion potential (E_{corr}), anodic (β_a), cathodic (β_c), polarization resistance (R_p), the inhibition efficiency (%IE) and the rates of corrosion (CR) in absence and presence the inhibitors molecules in NaCl 3.5% solution (artificial seawater). Tafel plot reveals that E_{corr} for carbon steel or stainless steel in the presence of the inhibitors (50 ml of inhibitor was added) shifts to a higher (noble) position compared with blank solution, which means the protection works as anodic protection. The inhibition efficiency (%IE) was calculated by the following Eq.1⁵.

$$IE\% = \frac{(i_{corr})_o - (i_{corr})}{(i_{corr})_o} * 100 \quad \text{----- 1}$$

Where $(i_{corr})_o$ is the corrosion current density in the absence of inhibitors (blank), (i_{corr}) is the corrosion current density in the presence of inhibitors (100 ppm) (50 ml of inhibitor was added).

R_p in $\Omega \cdot \text{cm}^2$ was calculated from the Stern-Geary Eq. 2¹⁶:

$$R_p = B / i_{corr} \quad \text{----- 2}$$

$$B = \frac{\beta_a * \beta_c}{2.303 (\beta_a + \beta_c)} \quad \text{----- 3}$$

Where; R_p is the polarization resistance in $\Omega \cdot \text{cm}^2$, i_{corr} is the corrosion current density, β_a , and β_c are the anodic and cathodic Tafel slopes in V.dec.

The rates of corrosion, it is calculated by Faraday's law⁹ at four temperatures for carbon steel and stainless steel alloys without and with the inhibitor.

$$CR = 0.13 (e / d) i_{corr} \quad \text{----- 4}$$

Where (e) is the chemical equivalent of the metal, (d) its density, and i_{corr} is the corrosion current density at four temperatures. All the above-mentioned parameters that were calculated are shown in Table 2.

Table 2. Corrosion parameters for blank and inhibitor in NaCl solutions at different temperature ranges.

Material	T K°	E _{corr.} mv vs SCE	i _{cor} A/ cm ² x10 ⁻⁶	β _a (mV/Dec)	β _c (mV/ Dec)	R _p Ω.cm ²	CR(PL) mm.y ⁻¹	IE%
Blank + Carbon steel	293	-1.031	134.1	874	-735	1293	0.658	-
	303	-0.917	144.5	791	-192	463.9	0.709	-
	313	-0.880	153.9	739	-173	395.4	0.755	-
	323	-0.914	160.2	799	-185	406.4	0.786	-
Blank + Stainless steel	293	-0.117	75.23	111	-1123	526.5	0.399	-
	303	-0.121	79.8	124	928-	540.5	0.421	-
	313	-0.119	81.73	121	-1089	554.5	0.440	-
	323	-0.110	84.24	110	-118	259.5	0.467	-
Carbon steel+100 ppm of inhibitor	293	-0.593	10.95	85	126-	2011	0.054	92
	303	-0.634	13.75	122	174-	2272	0.067	91
	313	-0.654	14.50	129	211-	2394	0.071	91
	323	-0.645	18.65	152	259-	2233	0.092	89
Stainless steel+100 ppm of inhibitor	293	-0.266	1.793	456	-183	31625.75	0.004	98
	303	-0.227	3.902	604	173-	14965.14	0.004	96
	313	-0.226	4.147	1238	212-	18952.24	0.006	95
	323	-0.227	5.393	2960	-244	18149.5	0.007	94

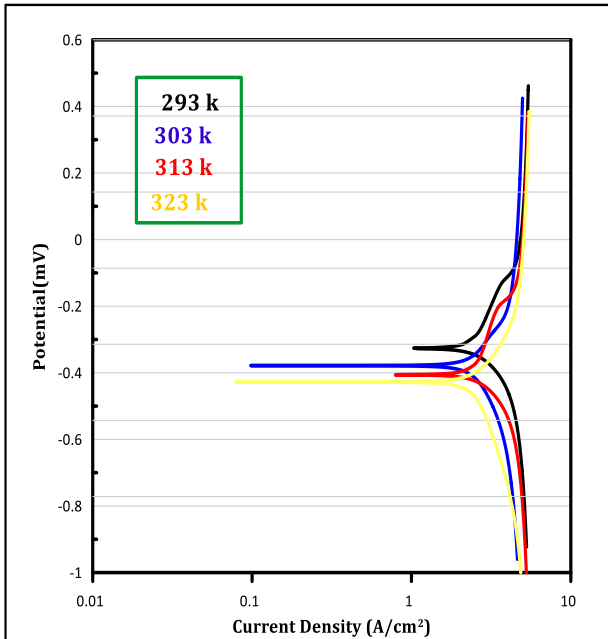


Figure 8. Polarization curves for corrosion of blank 3.5% NaCl solution (artificial seawater) at different temperatures (carbon steel).

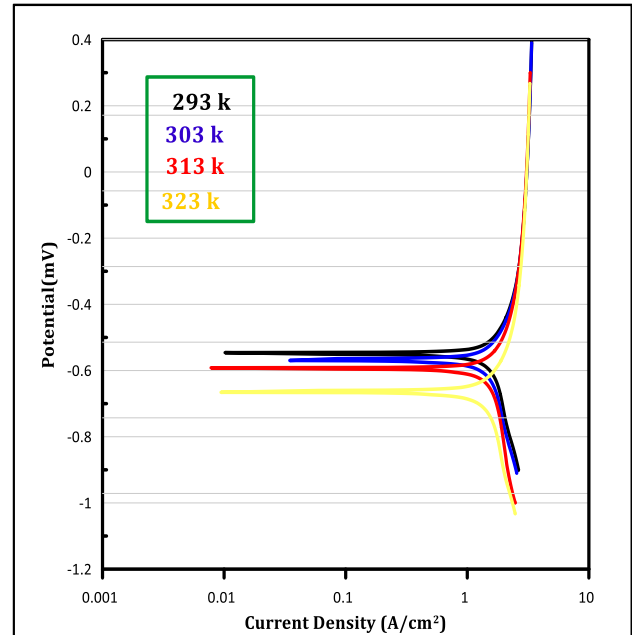


Figure 10. Polarization curves for corrosion of (carbon steel+100ppm of inhibitor) in 3.5% NaCl solution (artificial seawater) at different temperatures.

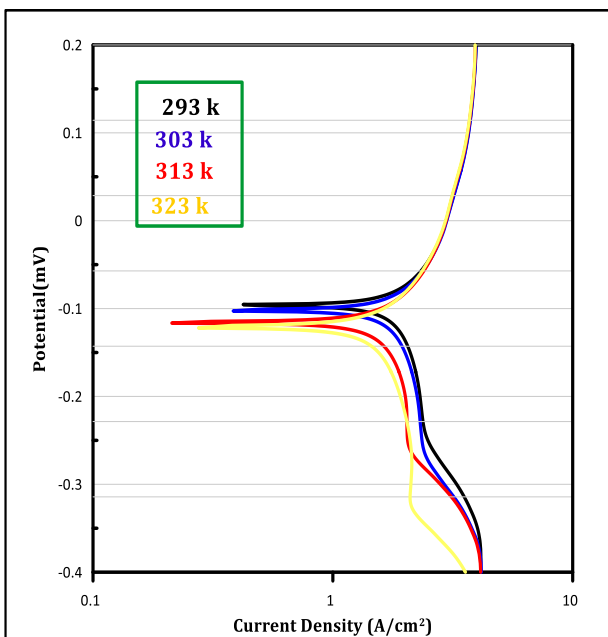


Figure 9. Polarization curves for corrosion of blank 3.5% NaCl solution (artificial seawater) at different temperatures (stainless steel).

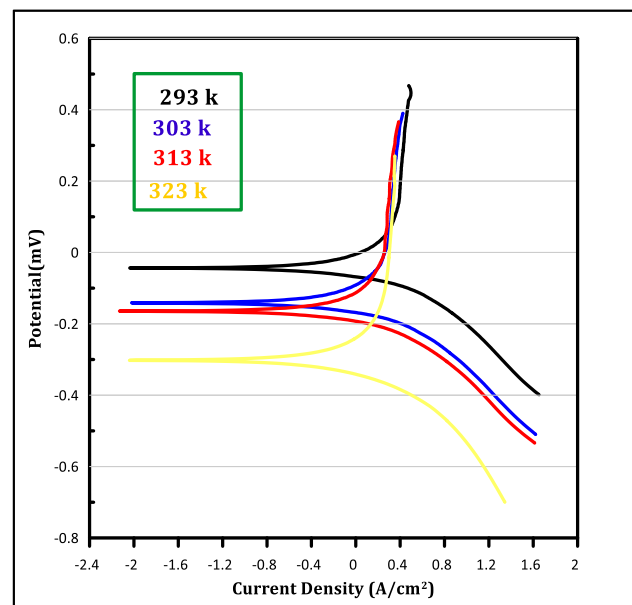


Figure 11. Polarization curves for corrosion of (stainless steel+100ppm of inhibitor) in 3.5% NaCl solution (artificial seawater) at different temperatures.

The data mentioned in the above Table 2 shows the following: We note that the corrosion current i_{corr} values increase with increasing temperature for the two alloys under study without and with the inhibitor, the reason is because corrosion is an electrochemical reaction and the rate of the reactions increases with increasing temperature. Also, a significant decrease in the values of the corrosion currents i_{corr} of the alloys is observed with the use of the inhibitor compared to the values without the use of the inhibitor, and this leads to a high inhibition efficiency. The polarization resistance values R_p of the two alloys without the use of the inhibitor decrease with increasing temperature, it is caused by the formation of a corrosion product (iron oxide), while the values of the polarization resistance of the alloys with the use of a high inhibitor (Schiff base) are greater than the values without the inhibitor and also decrease with increasing temperature, This explains why corrosion products are not formed on the surface of the alloys (carbon steel and stainless steel)¹. The values of corrosion rates for alloys without the inhibitor are high compared to the values when adding the inhibitor, and these values also increase with the increase in temperature, and this is due to the role of the inhibitor in reducing the corrosion process significantly (the inhibitor is adsorbed on the surface of the metal and forms an insulating layer that isolates the surface of the metal from the surroundings and stops the oxidation of the metal). Also, a significant decrease in the corrosion potential values of the alloys was observed when the inhibitor was added¹.

Kinetic and Thermodynamic parameters

The kinetic and thermodynamic values include: the activation energy (E_a), the entropy (ΔS^*), the enthalpy (ΔH^*), and the Gibbs free energy (ΔG^*). From Arrhenius plot Eq. 5¹⁰ estimated the activation energy (E_a) while the entropy (ΔS^*) and the enthalpy (ΔH^*) were estimated from derivative formulation Eq.6, called the transition state¹⁰.

$$\log i_{corr} = -\frac{E_a}{2.303 * R} \left[\frac{1}{T} \right] + \log A \quad \text{--- 5}$$

$$\log \left(\frac{i_{corr}}{T} \right) = \log \left(\frac{R}{Nh} \right) + \frac{\Delta S^*}{2.303R} - \frac{\Delta H^*}{2.303R} \left(\frac{1}{T} \right) \quad \text{--- 6}$$

From Eq. 7^{1,33} was estimated the Gibbs free energy (ΔG^*).

$$\Delta G^* = \Delta H^* - T\Delta S^* \quad \text{--- 7}$$

Where (i_{corr}) is the corrosion current density, h is the Planck's constant (6.626×10^{-34} J.s), N is Avogadro number (6.022×10^{23} Mol⁻¹), R is the universal gas constant (8.315 JK⁻¹mol⁻¹), T : Absolute temperature (K), ΔH^* is the enthalpy of activation, ΔS^* is the entropy of activation and ΔG^* is the Gibbs free energy. A plot of $\log (i_{corr})$ Vs $1/T$ of Eq. 5, provides straight lines with a slope of ($-E_a / 2.303R$) and an intercept of ($\log A$) for blank and with 100ppm inhibitor for two alloys carbon steel and stainless steel as shown in Fig. 12, 13, 14 and 15 respectively. A plot of $\log (i_{corr} / T)$ Vs $1/T$ of Eq. 6, provides straight lines with a slope of ($-\Delta H^*/2.303R$) and an intercept of ($\log R/Nh$) + $\Delta S^*/2.303R$) for blank and with 100ppm inhibitor for two alloys carbon steel and stainless steel as shown in Fig. 16, 17, 18 and 19 respectively. All the values of thermodynamics for the corrosion process of blank and inhibitor solutions for carbon steel and stainless steel at temperature range 293-323 K shown in Table 3.

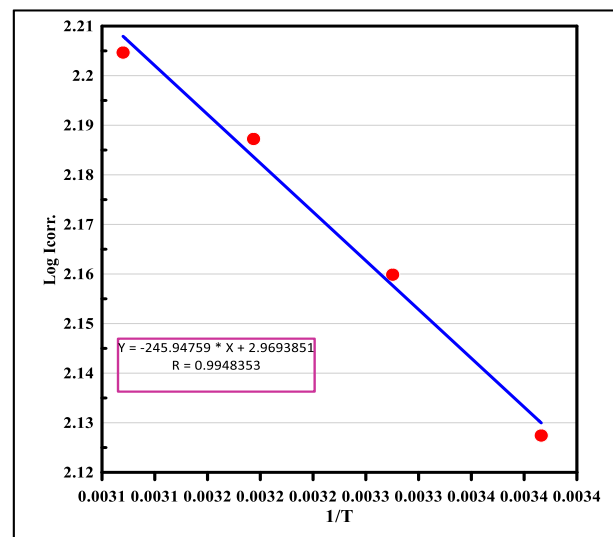


Figure 12. A Plot of $\log i_{corr}$ vs. $1/T$ for a blank + carbon steel in seawater at different temperatures.

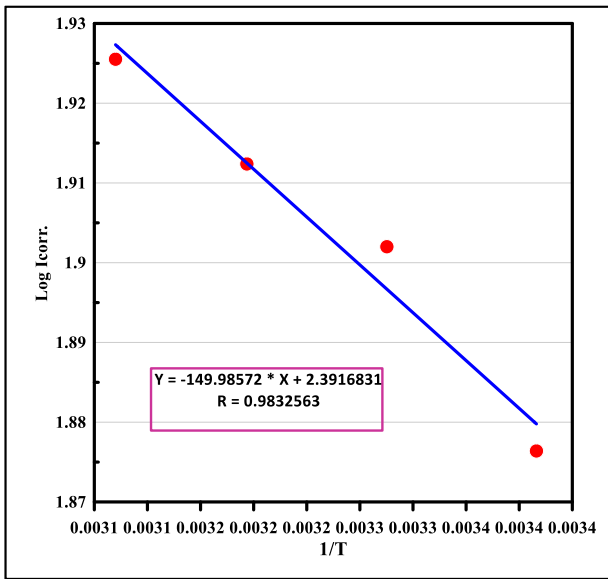


Figure 13. A Plot of $\log i_{corr}$ vs. $1/T$ for a blank + stainless steel in seawater at different temperatures.

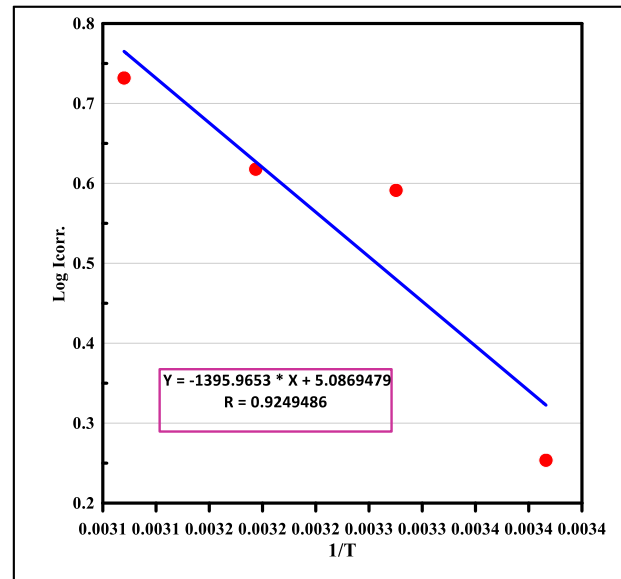


Figure 15. A Plot of $\log i_{corr}$ vs. $1/T$ for an inhibitor 100ppm (50 ml of inhibitor was added) + stainless steel in seawater at different temperatures.

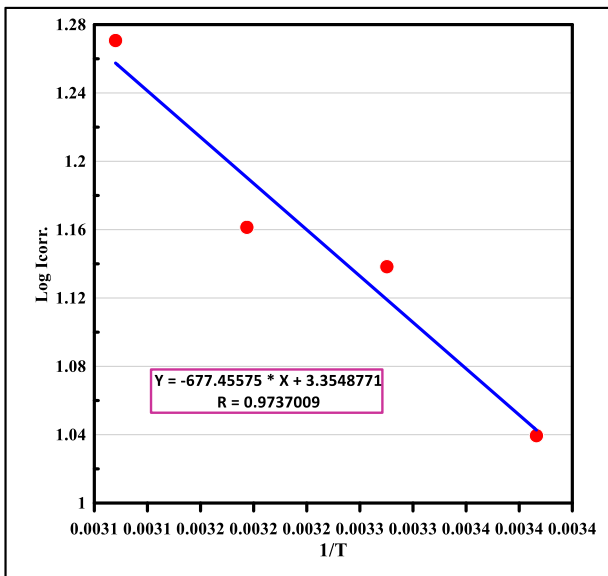


Figure 14. A Plot of $\log i_{corr}$ vs. $1/T$ for an inhibitor 100ppm(50 ml of inhibitor was added) + carbon steel in seawater at different temperatures.

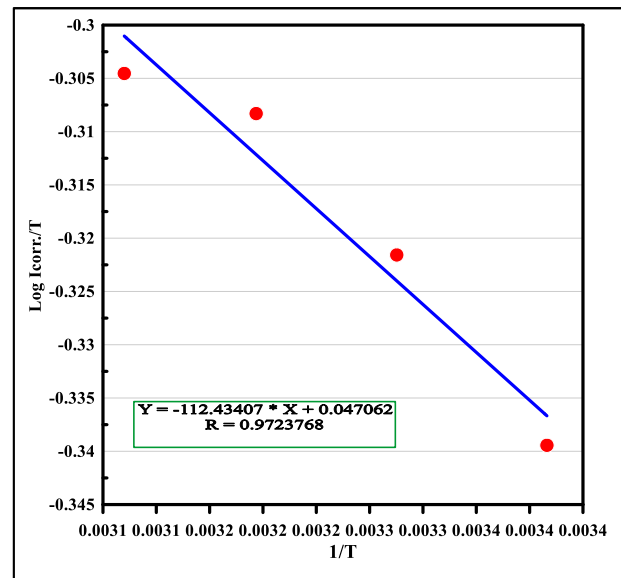


Figure 16. A Plot of $\log i_{corr}/T$ vs. $1/T$ for blank + carbon steel in seawater at different temperatures.

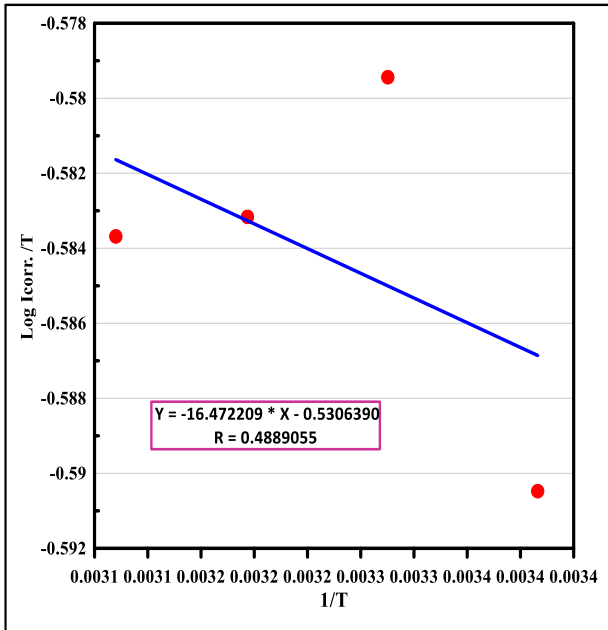


Figure 17. A Plot of $\log i_{corr.}/T$ vs. $1/T$ for blank + stainless steel in seawater at different temperatures.

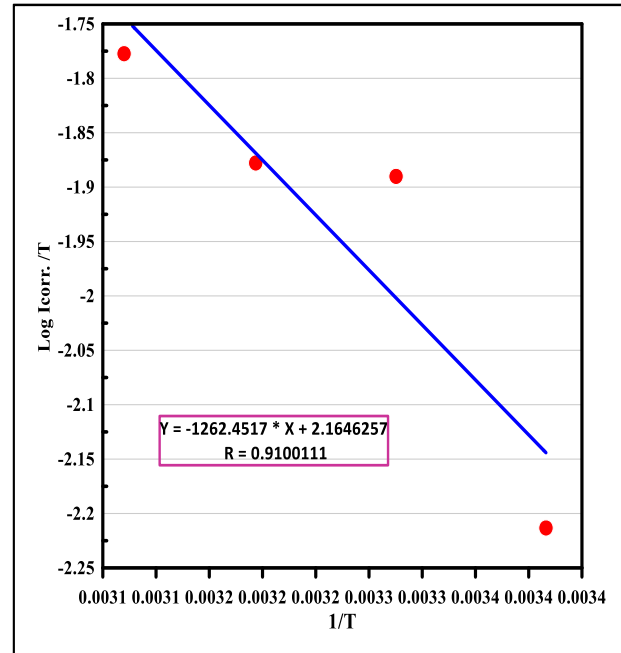


Figure 19. A Plot of $\log i_{corr.}/T$ vs. $1/T$ for an inhibitor 100ppm(50 ml of inhibitor was added) + stainless steel in seawater at different temperatures.

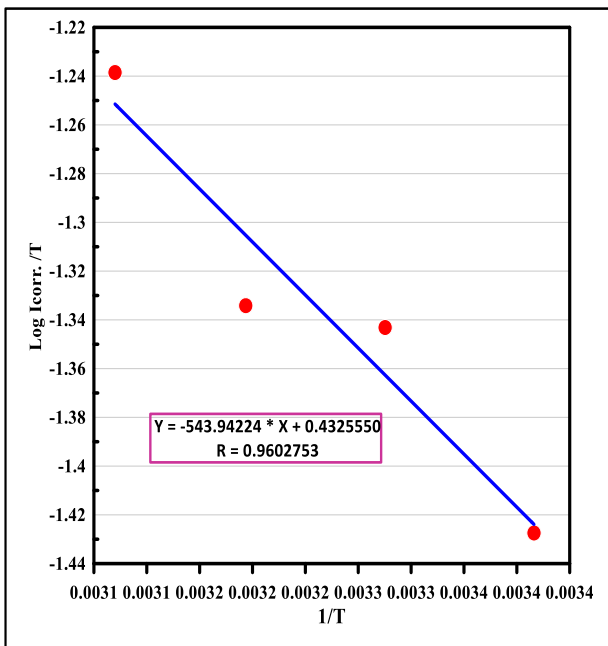


Figure 18. A Plot of $\log i_{corr.}/T$ vs. $1/T$ for an inhibitor 100ppm(50 ml of inhibitor was added) + carbon steel in seawater at different temperatures.

Table 3. The values of thermodynamics for the corrosion process of blank and inhibitor solutions for carbon steel and stainless steel at temperature range (293-323) K.

Sample	T(K°)	Ea (kJ/mole)	ΔH^* (kJ/mol)	ΔS^* (J/mol.K)	ΔG^* (kJ/mol)
Blank + Carbon steel	293	4.709	2.153	-197	59.87
	303				61.84
	313				63.81
	323				65.78
Blank + Stainless steel	293	2.872	0.315	-187	55.2
	303				57.06
	313				58.85
	323				60.72
Carbon steel +100 ppm of inhibitor	293	12.973	10.416	-189	65.79
	303				67.68
	313				69.57
	323				71.51
Stainless steel +100 ppm of inhibitor	293	26.733	24.176	-156	69.88
	303				71.44
	313				73.00
	323				74.56

The results are shown in the Table 3 above show facts that support the success of the inhibition process: The values of the activation energies of the alloys with the use of the inhibitor are much higher than their values without the inhibitor and this is due to the increase of the inhibitor molecules covering the surface of the metal ¹. Inhibitors in aqueous solutions alter the corrosion reaction kinetics by suggesting a different reaction pathway with lower activation energies, and this behavior is beneficial in inhibiting the corrosion rate of metal ¹. It was also noticed that the values of the activation enthalpy of the stainless steel alloy increased with the use of the inhibitor more than of the finding in the values of the activation enthalpy of carbon steel, and this supports that the inhibition efficiency of the stainless steel alloy is higher than the inhibition efficiency of the carbon steel alloy. The enthalpy of activation for the transition process takes positive values, and this indicates that the corrosion reaction is endothermic. Chemical adsorption requires activation energy values of more than 80 KJ/mol and since the activation energy values for the metals

under study showed less than 80 KJ/mol (from 10KJ/mol to 24 KJ/mol), this indicates that it is a physical adsorption ¹⁰. The action of the inhibitor in reducing metal corrosion is its physical adsorption on the surface of the metal and it forms an insulating layer on the surface of the metal isolating it from the environment causing the corrosion and prevents the oxidation of the metal.

There is further evidence that it is physical adsorption is the enthalpy (ΔH^*) values of less than 40 KJ/mol for the studied metals, because when the enthalpy values are 100 KJ/mol, the adsorption is chemical ¹⁰. The values of ΔS^* for in the presence and absence of the inhibitor are negative, this means that the activated complex, which is the rate-limiting step of the reaction, represents an association rather than a dissociation, this indicates a decrease in disorder taking place by going from the reactants to the activated complex ¹⁰. The values of activation Gibbs free (ΔG^*) energies take positive values and most of them change slightly with increasing temperature, and this indicates that

the activated complex is unstable and the probability of its formation decreases with increasing temperature, it also describes that the

process is non-spontaneous one for transition reaction ⁵.

Conclusion

Through this work, the significant effect of the inhibitor was observed in reducing corrosion of the two metals, stainless steel and carbon steel, with high reinforcement of corrosion protection when

using a concentration of 100ppm and at temperatures from 20 – 50C° this is supported by the thermodynamic kinetic properties of the inhibition process.

Acknowledgment

The author thanks Dr. Haider, director of the continuing education center at the University Al-Turath College, for stealth check for search, and

lecturer Ziad Mohsen Bandar, lecturer in University Al-Turath College, for his high efforts in proofreading the research.

Author's Declaration

- Conflicts of Interest: None.
- We hereby confirm that all the Figures and Tables in the manuscript are mine/ours. Furthermore, any Figures and images, that are not ours, have been included with the necessary permission for re-publication, which is attached to the manuscript.

- The author has signed an animal welfare statement.
- Authors sign on ethical consideration's approval.
- Ethical Clearance: The project was approved by the local ethical committee in University of Baghdad.

Author's Contribution Statement

This work was carried out in collaboration between all authors. M H the owner of the research idea and made measurements of corrosion with wrote and

edited the manuscript. N A, made measurements of corrosion with revisions idea. T H, S R, and Sh M, prepared of inhibitor. H H, Check the linguistics.

References

1. Rehan A, Lami N, Khudhair N. Synthesis, Characterization and Anti-corrosion Activity of New Triazole, Thiadiazole and Thiazole Derivatives Containing Imidazo[1,2-a]pyrimidine Moiety. *Chem Methodol.* 2021; 5(4): 285-295. <https://doi.org/10.22034/chemm.2021.130448>.
2. Misawa T, Kyuno T, Suetaka W, Shimodaira S. The mechanism of atmospheric rusting and the effect of Cu and P on the rust formation of low alloy steels. *Corros Sci.* 1971; 11(1): 35-48. [https://doi.org/10.1016/S0010-938X\(71\)80072-0](https://doi.org/10.1016/S0010-938X(71)80072-0).
3. Maryam A, Sahar P, Abdollah A. Corrosion resistance and photocatalytic activity evaluation of electrophoretically deposited TiO₂-rGO nanocomposite on 316L stainless steel substrate. *J Ceramint.* 2019; 45(11): 13747-13760. <https://doi.org/10.1016/j.ceramint.2019.04.071>.
4. Gallegos M, Serna S, Lázaro I, Gutiérrez J, Mercado H, Arcos H, et al. Potentiodynamic polarization performance of a novel composite coating system of Al₂O₃/chitosan-sodium alginate, applied on an aluminum AA6063 alloy for protection in a chloride ions environment. *Coatings.* 2020; 10(1): 1-17. <https://doi.org/10.3390/coatings10010045>.
5. Khudhair A, Al-Sammaraei A. Enhancing of corrosion protection of steel rebar in concrete using TiO₂ nanoparticles as additive. *Iraqi J Sci.* 2019; 60(9): 1898-1903. <https://doi.org/10.24996/ijs.2019.60.9.2>
6. Saed A, Abdulkareem A. Anticorrosion behavior of deposited nanostructured polythiophene on stainless steel carbon steel and aluminum in sea water. *Int J Eng Res Sci.* 2016; 2(3): 1-7.
7. Mohammed F, Moustafa M, Marwa F, Ahmed H. Evaluation of synthesized polyaniline nanofibres as

- corrosion protection film coating on copper substrate by electrophoretic deposition. *J Mater Sci.* 2022; 57(3): 6085–6101. <https://doi.org/10.1007/s10853-022-06994-3>.
8. Karthika Sh, Jayadev, Kalyan R, Ananda M. Evaluation of Electrochemical and Anticorrosion Properties of Polyaniline-Fly Ash Nanocomposite. *Int J Corros.* 2021; 2021 (1547384): 1-10. <https://doi.org/10.1155/2021/1547384>.
 9. Al-Sammarraei M, Mazin R. Reduced Graphene Oxide Coating for Corrosion Protection Enhancement of Carbon Steel in Sea water. *Iraqi J Sci.* 2016; (Special Issue, Part B): 243-250.
 10. Al-Sammarraei M, Mazin R. Electrodeposited Reduced Graphene Oxide Films on Stainless Steel, Copper, and Aluminum for Corrosion Protection Enhancement. *Int J Corros.* 2017; 2017 (6939354): 1-8. <https://doi.org/10.1155/2017/6939354>.
 11. Le B, Xinli L, Dezhi W. Electrophoretic deposition of graphene coating as a corrosion inhibitor for copper in NaCl solution. *Res Surf Interfaces* . 2022; 8(100077): 1-6. <https://doi.org/10.1016/j.rsurfi.2022.100077>.
 12. Yang S, Zhuo K, Sun D, Wang X, Wang J. Preparation of graphene by exfoliating graphite in aqueous fulvic acid solution and its application in corrosion protection of aluminum. *J Colloid Interface Sci.* 2019; 543(7419): 263-272. <https://doi.org/10.1016/j.jcis.2019.02.068>.
 13. Zeena Sh, Abeer K, Taghried A. Study the Inhibition Effect of Amoxicillin Drug for Corrosion of Carbon Steel in Saline Media. *Baghdad Sci J.* 2022; 19(1): 121-131. <https://doi.org/10.21123/bsj.2022.19.1.0121>.
 14. Rasha A, Nafeesa J, Halah J, Ahlam M. Effect of Orphenadrine Citrate Drug on Corrosion of 316L Stainless Steel in Hydrochloric Acid. *Baghdad Sci J.* 2022; 63(7): 2793-2803. <https://doi.org/10.24996/ijcs.2022.63.7.4>.
 15. Rasha A, Nafeesa J, Ahlam M. Experimental and Theoretical Study of Neomycin Sulfate as Corrosion Protection for Titanium in Acid Media. *Baghdad Sci J.* 2021; 18(2): 374-383. <https://doi.org/10.21123/bsj.2021.18.2.0374>.
 16. Farhan A M, Jassim R A, Mohamoed A A. Corrosion Protection of Carbon Steel By Voltaren Drug in Acid Media and Theoretical Studies. *Res J Pharm Biol Chem Sci.* 2018; 9(2): 705-715.
 17. Taghried A, Qusay A, Mohammed A, Ahmed A, Lina M, Abdul Amir H, et al. New environmental friendly corrosion inhibitor of mild steel in hydrochloric acid solution: Adsorption and thermal studies. *Cogent Eng.* 2020; 7(1): 1-17. <https://doi.org/10.1080/23311916.2020.1826077>.
 18. Kadhim A, Al-Amiery A, Alazawi R, Al-Ghezi M, Abass R. Corrosion inhibitors. A review. *Int J Corros Scale Inhib.* 2021; 10(1): 54–67. <https://doi.org/10.17675/2305-6894-2021-10-1-3>.
 19. Hanoon M, Resen M, Al-Amiery A, Kadhum H, Takriff S. Theoretical and Experimental Studies on the Corrosion Inhibition Potentials of 2-((6-Methyl-2-Ketoquinolin-3-yl)Methylene) Hydrazinecarbothioamide for Mild Steel in 1 M HCl. *Prog. Color Colorants Coat.* 2022; 15(1): 21-33. <https://doi.org/10.30509/pccc.2020.166739.1095>.
 20. Yasir M, Eltmimi A, Alhabeeb S, May H. Experimental and theoretical investigations on the inhibition efficiency of N-(2,4-dihydroxytolueneylidene)-4-methylpyridin-2-amine for the corrosion of mild steel in hydrochloric acid. *Int J Corros Scale Inhib.* 2021; 10(3): 885–899. <https://doi.org/10.17675/2305-6894-2021-10-3-3>.
 21. Mustafa M, Sayyid F, Betti N, shaker L, Hanoon M, Alamiery A, et al. Inhibition of mild steel corrosion in hydrochloric acid environment by 1-amino-2-mercapto-5-(4-(pyrrol-1-yl)phenyl)-1,3,4-triazole. *S Afr J Chem Eng* 2022; 39(11): 42-51. <https://doi.org/10.1016/j.sajce.2021.11.009>.
 22. Festus C, Odozi W, Olakunle M. Preparation, Spectral Characterization and Corrosion Inhibition Studies of (E)-N-{(Thiophene-2-yl)methylene}pyrazine-2-carboxamide Schiff Base Ligand. *Protect Met.* 2020; 56(3): 651-662. <https://doi.org/10.1134/S2070205120030107>.
 23. Bhaskara Sh, Fakrudeen P, Desalegn T, Murthy A, Bheemaraju V. Evaluation of Corrosion Inhibition Efficiency of Aluminum Alloy 2024 by Diaminostilbene and Azobenzene Schiff Bases in 1 M Hydrochloric Acid. *Int J Corros.* 2021; 2021(5869915): 1-20. <https://doi.org/10.1155/2021/5869915>.
 24. Bahaa S, Muna K, Mustafa K, Waleed K, Mahdi M, Mohammed H, et al. Corrosion Inhibition of Mild Steel in Hydrochloric Acid Environment Using Terephthaldehyde Based on Schiff Base: Gravimetric, Thermodynamic, and Computational Studies. *Molecules.* 2022; 27(4857): 1-19. <https://doi.org/10.3390/molecules27154857>.
 25. El-Bakri Y, Boudalia M, Echihi S, Harmaoui A, Sebhaoui J, Elmsellem H, et al. Performance and theoretical study on corrosion inhibition of new Triazolopyrimidine derivative for carbon steel in the corrosion of carbon steel in sea water. *Iraq J Sci.* 2019; 60(4): 688-705.
 26. Rehab K, Suaad H, Athraa A. Synthesis, identification, theoretical and experimental studies for carbon steel corrosion inhibition in seawater for new urea and thiourea derivatives linkage to 5-nitro isatin moiety. *Der Phar Chem.* 2018; 10(7): 86-99.
 27. Salman T, Zinad D, Jaber H, Al-Ghezi M, Mahal A, Takriff M, et al. Effect of 1,3,4-Thiadiazole Scaffold on the Corrosion Inhibition of Mild Steel in Acidic Medium: An Experimental and Computational

- Study. *J Bio Tribocorros*. 2019; 5(2): 1-11. <https://www.doi.org/10.1007/S40735-019-0243-7>.
28. Rehab M, Mustafa Al. Theoretical and Experimental Study of Corrosion Behavior of Carbon Steel Surface in 3.5% NaCl and 0.5 M HCl with Different Concentrations of Quinolin2-One Derivative. *Baghdad Sci J*. 2022; 19(1): 105-120. <https://doi.org/10.21123/bsj.2022.19.1.0105>.
29. Rehab M, Mustafa A, Luma S. DFT Calculations and Experimental Study to Inhibit Carbon Steel Corrosion in Saline Solution by Quinoline-2-One Derivative. *Baghdad Sci J*. 2020; 18(1): 113-123. <https://doi.org/10.21123/bsj.2021.18.1.0113>.
30. Rasha A, Muna S, Ahlam M. Protection of Galvanized steel from corrosion in salt media using sulfur. *Baghdad Sci J*. 2022; 19(2): 347-354. <https://dx.doi.org/10.21123/bsj.2022.19.2.0347>.
31. Mansfeld F. Tafel slopes and corrosion rates from polarization resistance measurements. *Corrosion*. 1973; 29(10): 397-402. <https://doi.org/10.5006/0010-9312-29.10.397>.
32. Kiani M, Mousavi M, Mousavi S, Shamsipur M, Kazemi S. Inhibitory effect of some amino acids on corrosion of Pb-Ca-Sn alloy in sulfuric acid solution. *Corros Sci*. 2008; 50(4): 1035-1045. <https://doi.org/10.1016/j.corsci.2007.11.031>.
33. Paul S, Van Z. Corrosion deterioration of steel in cracked SHCC. *Int J Concr Struct Mater*. 2017; 11(3):557-572. <https://doi.org/10.1007/s40069-017-0205-8>.
34. Rashd M, Musa A, Farah W, Bulgasem Y. Synthesis, Characterization and Antibacterial Activity of Schiff Bases Derived from 4-Dimethylaminobenzaldehyde with Some Amino Acids and 4-Aminoantipyrine toward Cu (II), Ni (II), Co (II), Cd (II) and Mn (II) Ions. *IOSR J Appl Chem*. 2017; 10(6): 6-13. <https://dx.doi.org/10.9790/5736-1006010613>

تعزيز الحماية من التآكل لمعدنين الكربون والفولاذ المقاوم للصدأ باستخدام مثبط (قاعدة شيف) في ماء المالح

مازن حسن رحيمة¹، نور علي خضير²، تغريد هاشم النور³، سلام رياض العايش³، حسين حسن خرنوب⁴ و شذى محمد حسن³

¹قسم طب الأسنان، كلية التراث الجامعة، بغداد، العراق.

²قسم الكيمياء، كلية العلوم، جامعة بغداد، بغداد، العراق.

³قسم الكيمياء، كلية التربية للعلوم الصرفة ابن الهيثم، جامعة بغداد، بغداد، العراق.

⁴قسم التدوير والعناية المركزة، كلية التراث الجامعة، بغداد، العراق.

الخلاصة

قدم هذا البحث حلاً للمشكلة التي تواجه السبائك وهي مشكلة التآكل بتقليل التآكل وتعزيز الحماية باستخدام مثبط (قاعدة شيف). تم تحضير المثبط (قاعدة شيف) عن طريق تفاعل مواد الاولية (4-ثنائي ميثيل أمينوبنزالديهايد و 4-أمينو أنتيبيرين). تم تشخيصه بواسطة تقنية اشعة تحت الحمراء , حيث أثبت طيف الأشعة تحت الحمراء ومن خلال الحزم الواضحة أن قاعدة شيف قد تشكلت بشكل جيد وبنقاوة عالية. تمت دراسة سلوك التآكل للفولاذ الكربوني والفولاذ المقاوم للصدأ في وسط ملحي (ماء بحر صناعي 3.5% كلوريد الصوديوم) قبل وبعد استخدام المثبط عند أربع درجات حرارة: 20 ، 30 ، 40 ، و 50 درجة مئوية باستخدام ثلاثة أقطاب المجهاد الساكن. تمت دراسة سلوك التآكل بواسطة استقطاب الكاثود والأنود الذي تم من خلاله فحص جميع معاملات التآكل والتي تشمل: تيار التآكل (1341 × 10⁻⁷ - 5393 × 10⁻⁹ , جهد التآكل (-1.031 - -0.227) SCE vs mV , معدلات التآكل (0.007-0.658 mm.y⁻¹), نسبة كفاءة التثبيت (92-98%), وطاقة التنشيط (4.709-26.733 كيلو جول/مول). تمت أيضاً دراسة الخصائص الديناميكية الحرارية والحركية لسلوك التآكل لهذين المعدنين قيد الدراسة ، والتي تشمل الانتالبي الحراري (2.153-24.176 كيلو جول/مول، الانتروبي(-197 - -156 كيلو جول/مول), وطاقة جيبس الحرة (59.87-74.56 كيلو جول/مول) قبل وبعد اضافة المثبط.

الكلمات المفتاحية: تثبيط التآكل، حديد الكربوني، مثبط، قاعدة شيف، حديد الفولاذ المقاوم للصدأ.